

Tectonic and climatic controls of denudation rates in active orogens: The San Bernardino Mountains, California

Steven A. Binnie^{a,*}, William M. Phillips^{b,1}, Michael A. Summerfield^b, L. Keith Fifield^c, James A. Spotila^d

^a University of California, Berkeley Space Sciences Lab 7 Gauss Way Berkeley, CA 94720-7450, USA

^b Institute of Geography, School of GeoSciences, University of Edinburgh, Drummond St., Edinburgh, EH8 9XP, UK

^c Department of Nuclear Physics, Research School of Physical Sciences and Engineering, The Australian National University, Canberra ACT 0200, Australia

^d Department of Geological Sciences, Virginia Polytechnic Institute and State University, 4044 Derring Hall (0420) Blacksburg, VA 24061, USA

ARTICLE INFO

Article history:

Received 1 June 2009

Received in revised form 5 January 2010

Accepted 10 January 2010

Available online 22 January 2010

Keywords:

Denudation rates

Erosion rates

Cosmogenic ¹⁰Be

Landscape evolution

Climate

Tectonics

ABSTRACT

The relative importance of climatic and tectonic factors in driving rates of denudation in mountain ranges has long been debated, with both precipitation and rates of crustal uplift cited as first order controls in a variety of different mountainous settings. Few studies, however, have explicitly considered the influence of climatic and tectonic processes on denudation rates during the early stages of orogenesis. Using basin-wide denudation rates derived from in-situ cosmogenic ¹⁰Be, and published modern precipitation rate data, the significance of rainfall and snowfall on rates of denudation is evaluated for the San Bernardino Mountains, California. Denudation rates vary between 52 mm ka⁻¹ in the arid northern regions of the mountains and 2700 mm ka⁻¹ in the more humid southern sector. We select three basins where the influence of precipitation on denudation rates can be isolated from the effects of crustal uplift and find that there is no apparent relationship between denudation rates and precipitation. Denudation rates differ more than five-fold on the opposing slopes of Mill Creek, a valley bisected by a major splay of the San Andreas Fault, and we propose that this denudation rate disparity can be best explained by variations in uplift rates across the fault. The results suggest that crustal uplift is the mechanism that underpins the ~50-fold variability in denudation rates we have measured in the San Bernardino Mountains, but that this must be facilitated by sufficient precipitation to remove valley-fill deposits.

© 2010 Elsevier B.V. All rights reserved.

1. Introduction

Interactions and feedbacks between tectonics and climate are considered to create relief and drive denudation across a broad range of spatial and temporal scales. However, due to the difficulties inherent in obtaining data over appropriate scales in settings where variables can be well constrained, the relationships between climate, tectonic displacement and rates of denudation remain unclear (Whipple, 2009). In mountainous terrains, base-level lowering controls bedrock channel incision and limits the long-term denudation rates of the surrounding topography. Modelling and field studies indicate that rates of bedrock channel incision will be dictated by a function of channel gradient and volume of discharge, implying that tectonic uplift or precipitation are responsible for rates of denudation (Howard and Kerby, 1983; Seidl et al., 1994; Whipple and Tucker, 1999).

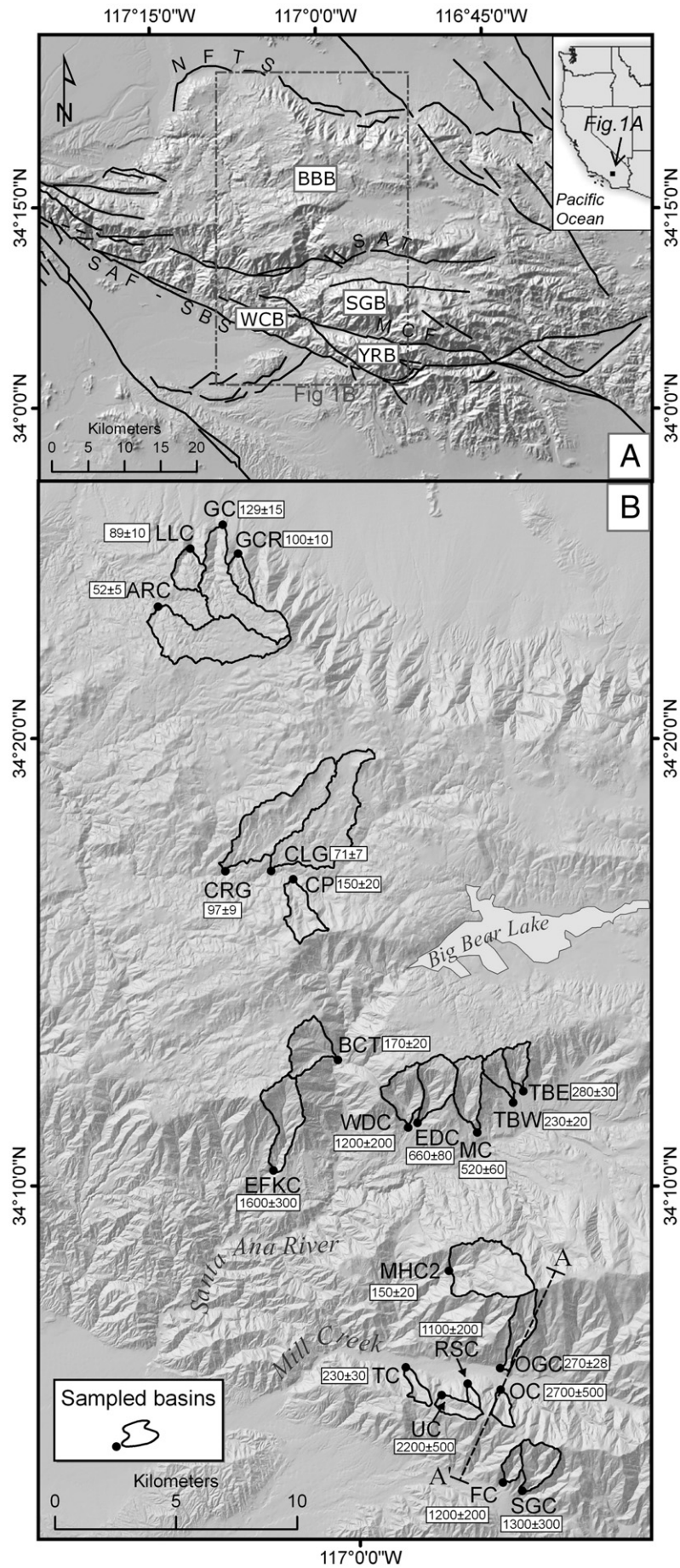
Whereas channel width adjustments and the role of suspended sediment may complicate a simple interpretation (Hartshorn et al., 2002; Whittaker et al., 2007), several recent studies have provided support for a climatic control of denudation rates using correlations with measured rates or inferred patterns of precipitation (e.g. Montgomery et al., 2001; Harris and Mix, 2002; Reiners et al., 2003; Wobus et al., 2003; Thiede et al., 2004; Grujic et al., 2006; Huntington et al., 2006). Other workers have highlighted the lack of a relationship between climate and denudation rates and have instead suggested a tectonic control (Riebe et al., 2001b), an assertion supported by studies that imply that crustal displacement coincides with rapid denudation in mountainous environments (e.g. Burbank et al., 2003; Vance et al., 2003; Malusa and Vezzoli, 2006). While some have suggested that it is the temporal and spatial coincidence of various climatic, tectonic and lithological variables that focuses rapid rates of denudation (e.g. Hovius, 2000; Dadson et al., 2003) there is little consensus as to how, and to what extent, climatic variables and crustal displacement influence denudation rates.

In studies of what drives denudation in mountainous settings, few have explicitly considered the controls of denudation during the early stages of orogenesis. During this period topography and drainages respond to changing base levels and so vital insights into the relative

* Corresponding author. Tel.: +1 510 643 7629; fax: +1 510 643 1433.

E-mail addresses: sbinnie@ssl.berkeley.edu (S.A. Binnie), phillips@uidaho.edu (W.M. Phillips), mas@geo.ed.ac.uk (M.A. Summerfield), keith.fifield@anu.edu.au (L.K. Fifield), spotila@vt.edu (J.A. Spotila).

¹ Present address: Idaho Geological Survey, University of Idaho, Moscow, Idaho, 83844, USA.



influence exerted by climate and tectonics on denudation rates may be gained by investigating this stage of mountain building. In this study we focus on the San Bernardino Mountains, a range in southern California where topography is considered to be responding to the early stages of fault block orogenesis (Dibblee, 1982; Spotila et al., 1998; Binnie et al., 2008). Previous studies in the San Bernardino Mountains have used ^{10}Be -derived denudation rates to investigate processes of alluvial sediment transport (Binnie et al., 2006), the existence of threshold topography (Binnie et al., 2007), and topographic development during the early-stages of fault-block orogenesis (Binnie et al., 2008). Here, we incorporate data from these previous works to present new insights into the factors which control rates of denudation in the San Bernardino Mountains. We do so by comparing denudation rates and modern climatic data in parts of the range where topography has not yet responded to the onset of orogenesis, allowing us to isolate the influence of precipitation. Next, we show how contrasting denudation rates across a major fault can best be explained by tectonically driven base-level change, and we consider the role that precipitation might play in such settings. We then discuss our findings in relation to the timescales over which measurements are made, specifically considering whether modern precipitation rate data are comparable with the averaging periods of the cosmogenic ^{10}Be -derived denudation rates, and whether it is appropriate to compare denudation rates derived using this technique with tectonic processes that operate over much longer time-frames. Finally, we consider the broader implications of our findings for other studies investigating denudation rate controls in orogens.

2. Study area

2.1. Geomorphology

The San Bernardino Mountains form part of the Transverse Ranges in southern California that have risen as a result of transpression across a section of the San Andreas Fault Zone. They extend approximately 100 km east to west, 80 km north to south and are composed of five crustal blocks. The broad Big Bear block dominates the northern and central parts of the range and has formed between two opposing reverse fault systems, the Northern Frontal Thrust System and the Santa Ana Thrust (Fig. 1A). Displacement on these faults is considered to have elevated the Big Bear block relative to its surroundings by the late Pliocene (May and Repenning, 1982; Meisling and Weldon, 1989). The northern and southern escarpments, which have formed above the surface traces of these fault systems, flank a broad plateau (<100 m relief over wavelengths of several kilometres) with an average elevation of ~1900 m. The bedrock on the plateau is principally granodiorite and quartz monzonite and much of the surface is mantled by a deeply weathered granitic horizon that can be traced northwards into the Mojave Desert, suggesting that the surfaces of the Big Bear block plateau and Mojave Desert were once contiguous (Oberlander, 1972; Dibblee, 1982; Meisling and Weldon, 1989; Spotila and Sieh, 2000). Remnants of basalt flows which pre-date the formation of the San Bernardino Mountains overlie the weathered granitic horizon, indicating that it formed before orogenesis and has undergone little denudation since then (Oberlander, 1972; Woodburne, 1975). Further support for the minimal modification of this surface comes from fluvially rounded quartzite pebbles with a Mojave Desert or eastern Big Bear block provenance which lie on top of the weathered horizon along the crests of interfluvies and, hence, must have been deposited by fluvial activity prior to mountain building (Sadler and Reeder, 1983). In addition, quantitative support for minimal denudation of the plateau is provided by cosmogenic ^{10}Be -derived denudation rates as low as several tens of

mm ka^{-1} (Binnie et al., 2008), and apatite (U–Th)/He ages that pre-date the onset of orogenesis (Spotila et al., 1998).

South of the Big Bear block, and separated from it by the intermontane structural low of the Santa Ana Valley, the San Gorgonio block is an east–west trending, smooth crested ridge of granitic and gneissic basement with a maximum elevation of 3506 m and a local relief that exceeds 2000 m (Fig. 1A). A deeply weathered granitic horizon overlain by fluvially rounded quartzite pebbles, similar to that found on the Big Bear block plateau, mantles some of the slopes at high elevations on the San Gorgonio block, implying that the now more elevated slopes were once at the same elevation as the Big Bear block plateau and Mojave Desert, and that this palaeo-topography has not yet been stripped away (Spotila et al., 1998). This is consistent with the changes in topography at different elevations on the San Gorgonio block, where lower, steeper slopes display active debris chutes, shallow landsliding and evidence for past deep-seated slope failures, features typically absent from the more subdued topography at higher elevations. Although currently non-glaciated, some of the highest slopes of the San Gorgonio block display moraines, the dating of which suggests small cirque glaciers advanced at 20–18 ka, 16–15 ka, 13–12 ka and 9–5 ka ago (Owen et al., 2003). The timing of the formation of the San Gorgonio block is less well constrained than in other parts of the mountains but initiation of uplift ~3.3 Ma ago has been suggested based on the provenance of sedimentary deposits found in the Mojave Desert (Cox et al., 2003).

South of the San Gorgonio block is a narrow (<5 km wide) steep-sided ridge that is made up of the Yucaipa Ridge and Wilson Creek blocks (Fig. 1A). The Yucaipa Ridge block is the larger of the two with a maximum elevation of 2842 m and a local relief exceeding 1500 m. This block is bounded to the north by the high angle Mill Creek fault, which runs through the steep-sided valley containing Mill Creek, and to the south by the San Bernardino strand of the San Andreas fault zone (Allen, 1957; Yule and Sieh, 2003). The lithology of the block is predominately a highly fractured gneiss which appears to prevent significant deep-seated landsliding (Spotila et al., 2001; Morton et al., 2008), interspersed with patches of quartz monzonite. Thermochronometry indicates that the steep slopes of the Yucaipa Ridge block have undergone rapid denudation over the last ~1–2 Ma (Spotila et al., 2001), and the active debris chutes, rockfalls, and shallow landslips (Sadler and Morton, 1989) and recent debris flow activity (Morton et al., 2008) suggest that rapid denudation is continuing. The intermontane valley between the San Gorgonio and Yucaipa Ridge blocks forms the headwaters of the Mill Creek (Fig. 1B) and contains significant fill deposits. During higher flows this fill is transported and deposited in the wash along the southern range front of the mountains.

2.2. Climate of the San Bernardino Mountains

The present climate of the San Bernardino Mountains has a north–south gradient and varies strongly with altitude. Air masses associated with winter south–westerly storms are orographically elevated as they reach the Transverse Ranges providing more precipitation in the southern San Bernardino Mountains than in the north. Mean annual precipitation is of the order of 500 mm a^{-1} along the base of the slopes of the southern range front, and this increases to around 1000 mm a^{-1} along the crests of the southern peaks (Fig. 2A) (Minnich, 1986). At high elevations the majority of precipitation falls as snow (Fig. 2C), whereas below an altitude of ~1250 m snow is rare (Fig. 2B) (Minnich, 1989). In the summer months convective summer thunderstorms are common along the southern range front, but these tend to be localised and short-lived. In the northern part of the Big Bear block mean annual

Fig. 1. The study area showing (A) the principal structures of the San Bernardino Mountains discussed in the text. BBB Big Bear block; SGB San Gorgonio block; YRB Yucaipa Ridge block; WCB Wilson Creek block; NFTS North Frontal Thrust System; SAT Santa Ana Thrust; MCF Mill Creek fault; SAF–SBS San Andreas fault – San Bernardino Strand. (B) The location of cosmogenic samples and extents of basins measured with denudation rate results and 1σ uncertainties in mm ka^{-1} given in boxes next to each basin label. Transect A–A' through Mill Creek approximates the position of the cross sections shown in Fig. 6.

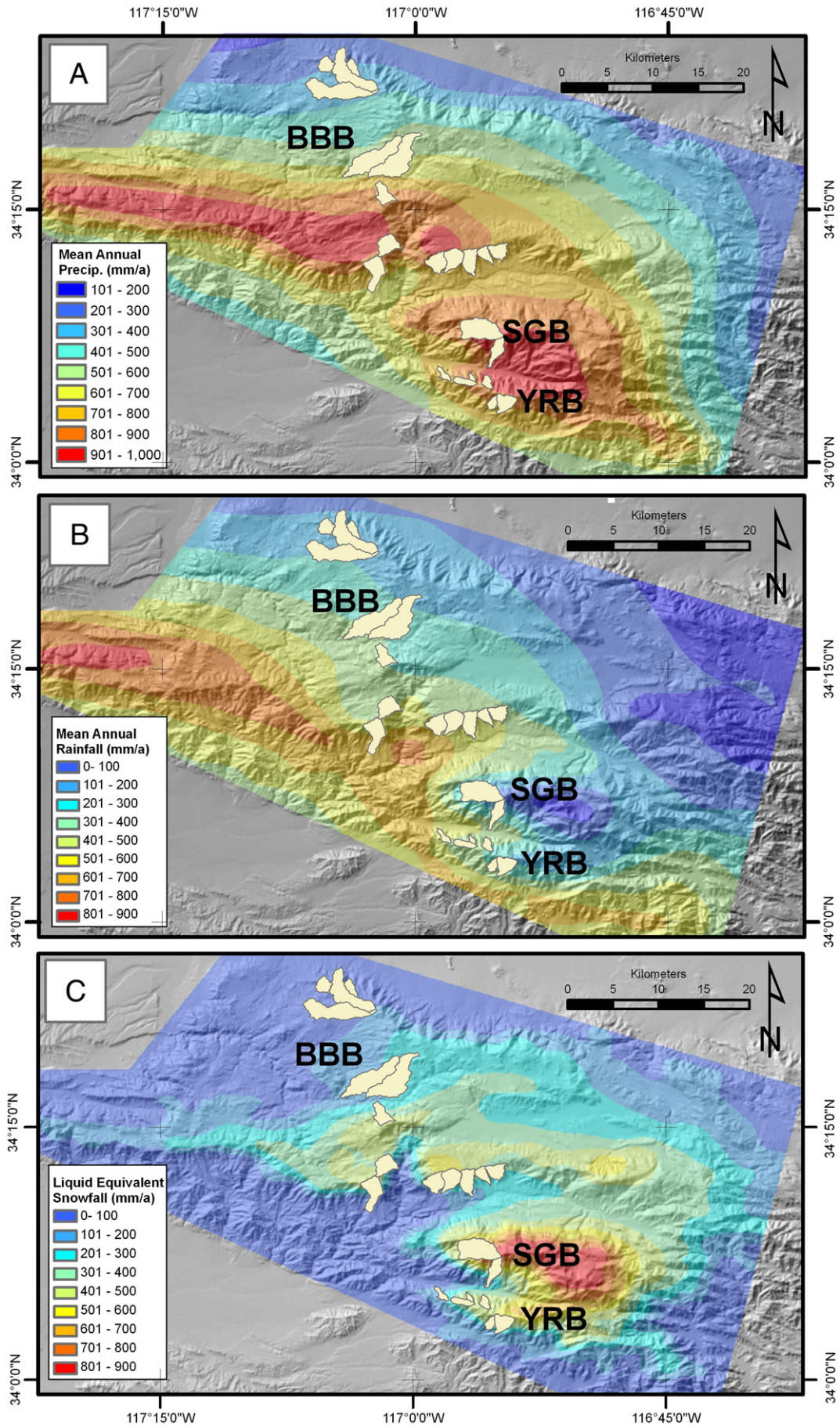


Table 1
Cosmogenic sample characteristics.

Sample ID	Latitude (d.d.)	Longitude (d.d.)	Spallation production rate scaling factor ^{a,c}	Muogenic production rate scaling factor ^{b,c}	Number of atoms ($\times 10^3$) $\pm 1\sigma$ (at g^{-1}) ^{d,e}	Denudation rate $\pm 1\sigma$ (mm ka^{-1}) ^{f,g}
UC	34.0845	−116.9685	3.6	2.0	5.6 \pm 1.1	2200 \pm 500
OC	34.0869	−116.9418	3.8	2.1	4.7 \pm 0.9	2700 \pm 500
SGC	34.0486	−116.9307	4.2	2.2	10.8 \pm 1.2	1300 \pm 300
FC	34.0532	−116.9393	3.8	2.1	10.1 \pm 1.1	1200 \pm 200
RSC	34.0894	−116.9554	3.6	2.0	11.0 \pm 1.2	1100 \pm 200
TC	34.0945	−116.9832	2.8	1.8	42.0 \pm 3.9	230 \pm 30
OGC	34.0935	−116.9400	5.2	2.6	62.1 \pm 3.2	270 \pm 28
MHC-2a	34.1299	−116.9610	5.5	2.7	151.7 \pm 17.4	130 \pm 20
MHC-2b	34.1299	−116.9610	5.5	2.7	120.0 \pm 11.1	160 \pm 21
MHC-2c	34.1299	−116.9610	5.5	2.7	120.6 \pm 10.8	160 \pm 21
MHC-2M ^h	–	–	–	–	–	150 \pm 20
WDC	34.1854	−116.9807	3.7	2.1	10.3 \pm 1.3	1200 \pm 200
EDC	34.1852	−116.9767	4.1	2.2	20.8 \pm 1.9	660 \pm 80
MC	34.1825	−116.9483	4.2	2.3	26.8 \pm 2.0	520 \pm 60
BCT	34.2083	−117.0123	3.8	2.1	74.4 \pm 5.2	170 \pm 20
EFKC	34.1702	−117.0567	3.5	2.0	7.7 \pm 1.3	1600 \pm 300
TBW	34.1926	−116.9318	4.3	2.3	62.0 \pm 3.0	230 \pm 20
TBE	34.1961	−116.9268	4.2	2.3	50.3 \pm 2.7	280 \pm 30
GCR	34.3940	−117.0544	3.1	1.7	100.9 \pm 6.1	100 \pm 10
LLC	34.3967	−117.0757	2.9	1.7	110.6 \pm 7.2	89 \pm 10
CP	34.2756	−117.0311	4.4	2.2	97.3 \pm 5.5	150 \pm 20
CRD	34.2787	−117.0631	3.7	2.0	127.7 \pm 5.8	97 \pm 9
CLG	34.2800	−117.0414	3.8	2.0	180.6 \pm 10.0	71 \pm 7
GC	34.4040	−117.0626	3.2	1.8	84.2 \pm 6.5	129 \pm 15
ARC	34.3748	−117.0914	3.3	1.8	215.1 \pm 9.4	52 \pm 5

^a Spallogenic production rate scaling factors include scaling for altitude and elevation following Stone (2000), and scaling for snow shielding following Gosse and Phillips (2001), using modern snowfall data from Minnich (1989).

^b Muogenic scaling factors include scaling for altitude and latitude according to Stone (2000).

^c Topographic shielding for each basin (S) is derived using $S = 1 - 3.6 \times 10^6 \alpha^{2.64}$ from Dunne et al. (1999), where α is the angle between the maximum and minimum basin elevations (see text for discussion).

^d Includes subtraction of atoms measured by laboratory blanks which typically had $^{10}\text{Be}/^9\text{Be}$ values of $\sim 1-2 \times 10^{-14}$ due to ^{10}Be inherent in the commercial ^9Be carrier used. Propagated uncertainty includes 1σ error on $^{10}\text{Be}/^9\text{Be}$ sample measurement and blank measurement, and 1% uncertainty on ^9Be carrier weights of sample and blank.

^e AMS measurement undertaken at the Australia National University, normalised to NIST SRM 4325 standard with an assumed $^{10}\text{Be}/^9\text{Be}$ of 3.0×10^{-11} .

^f Denudation rates derived using formulation and constants of Granger et al. (2001), which explicitly considers muogenic production. HSL spallogenic production rate is $5.1 \text{ at g}^{-1} \text{ a}^{-1}$ (Stone, 2000). 10% uncertainty assumed for production rates. Bedrock density is $2.6 \text{ g cm}^{-3} \pm 3\%$. Attenuation length for spallation is $160 \text{ cm}^2 \pm 4\%$. ^{10}Be half-life is 1.51 Ma.

^g The online CRONUS calculator does not cater for studies requiring spatially averaged production rates such as is required here (Balco et al., 2008). However, we have used the calculator to estimate what difference applying alternative scaling schemes would have on our results and find that the maximum difference in denudation rates between the scaling schemes used by the calculator is $< 4\%$, not large enough to influence any of our findings. In addition, while we incorporate no geomagnetic corrections, the difference including this would make to the denudation rates is estimated using the CRONUS calculator as a rate increase of $< 4\%$.

^h The denudation rate of MHC-2M is the average of MHC-2a, MHC-2b and MHC-2c, all of which were collected within several metres of each other. See Binnie et al. (2006) for more details.

precipitation is $< 200 \text{ mm a}^{-1}$. In these arid regions, where sparse vegetation encourages flash flooding, it is rare but extensive summer thunderstorms rather than winter pressure systems that are recognised as the more important agent of denudation (Minnich, 1989). Mean annual temperatures range from 13–21 °C at low elevations on the northern escarpment of the Big Bear block to 4–10 °C at high elevations on the San Gorgonio block (Miles and Goudie, 1997). Vegetation in the San Bernardino Mountains varies from juniper forests and chaparral in the northern Big Bear block region to desert grassland across the northern escarpment and into the Mojave Desert. The lower elevations of the southern Big Bear, the Yucaipa Ridge and San Gorgonio blocks are populated by mixed deciduous forest. Above 1500–1900 m mixed conifer and sub-alpine pine species dominate.

3. Methods

3.1. Cosmogenic ^{10}Be -derived denudation rates

Alluvial sediment samples from 22 basins were collected for the analysis of in-situ cosmic-ray-produced ^{10}Be along a north–south transect spanning the range of modern precipitation values found in

the San Bernardino Mountains (Fig. 1B). Collection and processing of these samples has been described elsewhere (Binnie et al., 2006, 2008), but we present this information here for completeness. To avoid a lithological bias on cosmogenic ^{10}Be production rates, and to exclude the influence of rock strength on the denudation rates measured, we selected basins which were predominantly homogeneous quartz-monzonite or gneiss. Basins displaying evidence for past glaciations were avoided (Owen et al., 2003), as were those where deep-seated landsliding or insufficient sediment mixing could potentially bias the cosmogenic analyses (Niemi et al., 2005; Binnie et al., 2006). There is evidence for shallow landsliding on the Yucaipa Ridge block, the southern escarpment of the Big Bear block and, at low elevations, on the San Gorgonio block, and this has the potential to introduce a grain size bias in cosmogenic analysis (Brown et al., 1995). However, no grain size bias was found in a previous study undertaken in a basin on the San Gorgonio block (Binnie et al., 2006) and, although we cannot discount the possibility that such a bias is present at other sample sites, it is very unlikely that the magnitude of this effect would be sufficient to influence our interpretations.

Alluvial samples were sieved to $< 20 \text{ mm}$, crushed and shaken in concentrated hydrochloric acid. Pure quartz separates were produced

Fig. 2. Maps illustrating the variability of (A) the mean annual precipitation, (B) the mean annual rainfall and (C) the mean annual liquid equivalent of snowfall in the San Bernardino Mountains (adapted from Minnich, 1989). BBB Big Bear block; SGB San Gorgonio block; YRB Yucaipa Ridge block. The location of the basins detailed in Fig. 1 is indicated. Colour figure available online.

using several leaches in a dilute hydrofluoric/nitric acid mixture according to Kohl and Nishiizumi (1992). The samples were spiked with a commercial ^9Be carrier (Spectrosol) and digested in hydrofluoric acid before repeated drying in the presence of perchloric acid. Ion exchange chromatography and precipitation were used to separate beryllium from other elements before dehydrating to beryllium oxide and pressing with silver. $^{10}\text{Be}/^9\text{Be}$ was measured by accelerator mass spectrometry at the Australian National University using the continuous beam monitor method of Middleton and Klein (1987). Measurements were normalised to the NIST SRM 4325 standard with an assumed $^{10}\text{Be}/^9\text{Be}$ value of 3.0×10^{-11} . Laboratory blanks were processed in tandem with the samples and their values were subtracted from the samples to give the ^{10}Be concentrations shown in Table 1.

The derivation of basin-averaged cosmogenic nuclide production rates must take into account the non-linear scaling of production rates with elevation. For low relief basins the mean basin elevation may give a sufficiently precise estimate of the spatially averaged production rate; however, in high-relief terrains the non-linear scaling of nuclide production with elevation may invalidate this approximation and basin hypsometry should be considered (Balco et al., 2008). Using the USGS National Elevation Dataset 1/3-arcsecond DEM for the region (approximately 10 m resolution) and ArcView commercial software we derived grids of spallogenic and muogenic production rate scaling factors following Stone (2000). The average values for each basin sampled were then calculated from these grids to give the muogenic and spallogenic production rate scaling factors (Table 1). Any decrease in production rates due to shielding by snow cover was estimated using modern snow-pack records (Minnich, 1989) and scaled according to equation 3.76 in Gosse and Phillips (2001) assuming six months cover by snow with a density of 0.24 g cm^{-3} . We assumed 10% uncertainties in both spallogenic and muogenic production rates to account for palaeomagnetic field fluctuations, changing amounts of snow shielding and variations in vegetation cover (e.g. Ferrier et al., 2005). Reductions in basin-wide

production rates due to topographic shielding by basin interfluves were approximated using equation 1 of Dunne et al. (1999) in conjunction with the DEM to estimate the maximum gradient at which a hypothetical planar surface would lie if draped across the divides (Binnie et al., 2006). Production rate decreases due to shielding by distant topography were estimated to be $<1\%$ and therefore ignored. Denudation rates were derived using the formulation and constants given in Granger et al. (2001) (Table 1). Selective mineral dissolution within soils may increase the residence times of quartz in regolith, biasing denudation rates (Riebe et al., 2001a). In the majority of the basins we sampled in the San Bernardino Mountains the rates are likely to be too rapid to be influenced by selective mineral dissolution. However, on the plateau and northern escarpment of the Big Bear block, rates are comparable with those of a study of Granger et al. (2001) where the effects of mineral dissolution decreased denudation rates by $<12\%$. In this study we do not account for mineral dissolution, hence the denudation rates from these regions should be considered as maxima. The 1σ uncertainty in our nuclide concentrations includes the propagated analytical uncertainty of the sample $^{10}\text{Be}/^9\text{Be}$ measurement, respective laboratory blank $^{10}\text{Be}/^9\text{Be}$ measurement, and a 1% analytical uncertainty in our ^9Be carrier mass determinations.

3.2. Precipitation values

The precipitation maps of Minnich (1986, 1989) use nearby profiles of freezing elevations, calibrated to the San Bernardino Mountains, along with several decades of precipitation data from a dense network of stations distributed throughout the mountains to interpolate mean annual rainfall and mean annual snowfall (liquid equivalent). These maps were digitised (Fig. 2) and the average value for each basin sampled was extracted from USGS National Elevation Dataset 1/3-arcsecond (approx 10 m resolution) DEM using ArcView commercial software (Table 2). Values for mean annual precipitation were obtained by the addition of the individual rainfall and snowfall

Table 2
Characteristics of sampled basins.

Basin ID	Lithology	Basin area (km ²) ^a	Basin averaged elevation (m) ^a	Mean basin hillslope gradient (°) ^a	Mean annual precipitation (mm a ⁻¹) ^b	Mean annual rainfall (mm a ⁻¹) ^b	Mean annual snowfall (mm a ⁻¹) ^b	Cosmogenic denudation rate $\pm 1\sigma$ (mm ka ⁻¹)	Cosmogenic denudation rate averaging period (ka) ^c
UC	Qtz – monzonite	1.1	1750	30.7	800 ± 160	470 ± 90	320 ± 60	2200 ± 500	1.0
OC	Gneiss	0.6	1750	35.4	880 ± 180	440 ± 90	440 ± 190	2700 ± 500	0.8
SGC	Gneiss	2.4	1800	37.0	820 ± 160	430 ± 90	390 ± 80	1300 ± 300	1.6
FC	Gneiss	0.9	1800	38.0	790 ± 160	500 ± 100	290 ± 60	1200 ± 200	1.9
RSC	Gneiss	0.3	1750	37.2	820 ± 160	430 ± 90	390 ± 80	1100 ± 200	2.0
TC	Gneiss	0.8	1520	25.3	740 ± 150	610 ± 120	130 ± 30	230 ± 30	10.4
OGC	Qtz – monzonite	2.2	2200	35.9	900 ± 180	440 ± 90	460 ± 90	270 ± 28	7.3
MHC-2M	Qtz – monzonite	5.8	2540	26.3	890 ± 180	280 ± 60	610 ± 120	150 ± 20	14.6
WDC	Qtz – monzonite	2.6	1600	32.2	850 ± 170	560 ± 110	290 ± 60	1200 ± 200	1.8
EDC	Qtz – monzonite	3.5	2060	28.1	870 ± 170	480 ± 100	390 ± 80	660 ± 80	3.3
MC	Qtz – monzonite	2.9	2100	26.5	830 ± 170	490 ± 100	340 ± 70	520 ± 60	4.1
BCT	Qtz – monzonite	3.1	1950	30.9	880 ± 178	610 ± 120	270 ± 50	170 ± 20	12.9
EFKC	Qtz – monzonite	4.1	1820	32.3	780 ± 160	540 ± 110	240 ± 50	1600 ± 300	1.4
TBW	Qtz – monzonite	1.6	1800	27.5	810 ± 160	470 ± 90	340 ± 70	230 ± 20	9.3
TBE	Qtz – monzonite	1.5	1800	28.4	800 ± 160	470 ± 90	320 ± 60	280 ± 30	7.7
GCR	Qtz – monzonite	1.2	1400	19.5	310 ± 60	270 ± 50	50 ± 10	100 ± 10	21.6
LLC	Qtz – monzonite	1.7	1540	18.4	300 ± 60	260 ± 50	40 ± 10	89 ± 10	25.6
CP	Qtz – monzonite	2.3	2200	21.6	820 ± 160	450 ± 90	370 ± 70	150 ± 20	13.8
CRD	Qtz – monzonite	7.7	2000	14.4	590 ± 12	420 ± 80	170 ± 30	97 ± 9	22.2
CLG	Qtz – monzonite	8.4	1970	9.7	620 ± 120	420 ± 80	200 ± 40	71 ± 7	29.9
GC	Qtz – monzonite	6.1	1690	16.8	330 ± 70	270 ± 50	70 ± 10	129 ± 15	17.1
ARC	Qtz – monzonite	7.6	1750	9.2	370 ± 70	290 ± 60	80 ± 20	52 ± 5	42.1

^a Derived from 10 m USGS National Elevation Dataset DEM data.

^b Uncertainties on all precipitation values assumed to be 20%.

^c Averaging period of the cosmogenic derived denudation rate is the time taken to erode a depth equivalent to the mean attenuation length, $\Lambda \rho^{-1}$ (where Λ is the absorption mean free path and ρ is rock density). The mean attenuation length of each sample is a function of the different penetration depths of nucleogenic and muogenic production, weighted by their relative contributions to the total nuclide inventory. The averaging periods should not be considered absolute lengths of time but indicate the timeframe over which the measured denudation rates are applicable (see Binnie et al., 2008, Appendix A, for a discussion of this point).

measurements. It is not possible to undertake rigorous error analysis of these values and so we apply a conservative 20% uncertainty to these estimates. Although absolute amounts of precipitation may have varied over the past few hundred to few thousand years, it is very likely that the spatial pattern in relative amounts of precipitation across the San Bernardino Mountains will have been conserved.

4. Results

Basin-averaged denudation rates are most rapid on the Yucaipa Ridge block, at low elevations on the San Gorgonio block, and on the southern escarpment of the Big Bear block. There is also a great deal of

variation in rates within these regions, with results ranging from 170–2700 mm ka⁻¹. This is in contrast with the much lower and less variable rates found on the plateau, the northern escarpment of the Big Bear block, and at high elevations on San Gorgonio block, where values range between 52 and 150 mm ka⁻¹. Basin averaged mean annual precipitation increases from north to south and is greater in basins at high elevations. However, the contribution of snowfall to the total mean annual precipitation also increases from north to south and with elevation (Fig. 2). The values for mean annual liquid equivalent of snowfall, mean annual rainfall and mean annual precipitation increase non-linearly as rates of denudation increase (Fig. 3).

We observe similar rates of denudation between the elevated basin MHC-2M on the San Gorgonio block (150 ± 20 mm ka⁻¹), basin CP in the southern Big Bear block (150 ± 20 mm ka⁻¹) and basin GC in the northern Big Bear block (129 ± 15 mm ka⁻¹) (Fig. 1). All three basins display remnants of the weathered surface considered to pre-date orogenesis, but they show a distinct difference in mean annual precipitation with values of 890 ± 180 mm a⁻¹ and 820 ± 160 mm a⁻¹ in basins MHC-2M and CP respectively, decreasing to 330 ± 70 mm a⁻¹ in basin GC. Plotting average basin hillslope gradients against denudation rates for all the basins sampled shows an approximately linear relationship where slopes are less than 30° (Fig. 4). Thus, we might expect that MHC-2M, with a mean slope gradient of 26.3°, would have a significantly greater rate of denudation than basin GC which has a mean slope gradient of 16.8°, or CP which has a mean slope of 21.6°. However, using the thermal offsets apparent in (U-Th)/He thermochronometric data, Spotila et al. (1998) suggest the San Gorgonio block has undergone ~10° of northward tilting, which has tilted the granite horizon to the north and may account for the increased average basin slope gradient in MHC-2M relative to that exhibited by GC. Both basins MHC-2M and GC have steeper lower reaches where the weathered horizon is absent, presumably as the pre-uplift low relief topography is being removed and base-level changes are propagating upstream. This rejuvenation is limited to the catchment mouths, with the majority of the surface area of both basins exhibiting the low relief pre-uplift surface, hence the contribution of the steeper topography to the basin-averaged denudation rates is probably limited.

Most of the precipitation falling at high elevations on the San Gorgonio block falls as snow, which with less immediate infiltration

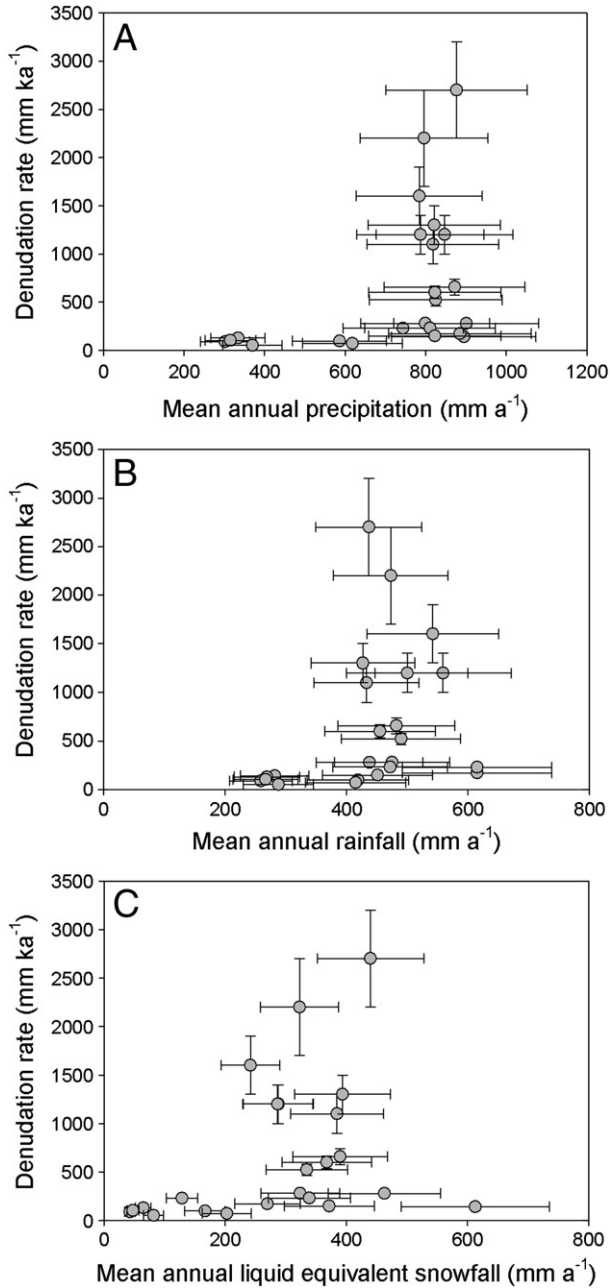


Fig. 3. Plots illustrating the relationship between basin-wide denudation rate and (A) mean annual precipitation, (B) mean annual rainfall and (C) mean annual liquid equivalent snowfall. While all three graphs appear to show increasing precipitation values correspond to increasing denudation rates a more detailed examination of selected basins where the influence of crustal displacement can be constrained reveals no correspondence between these variables. See text for discussion.

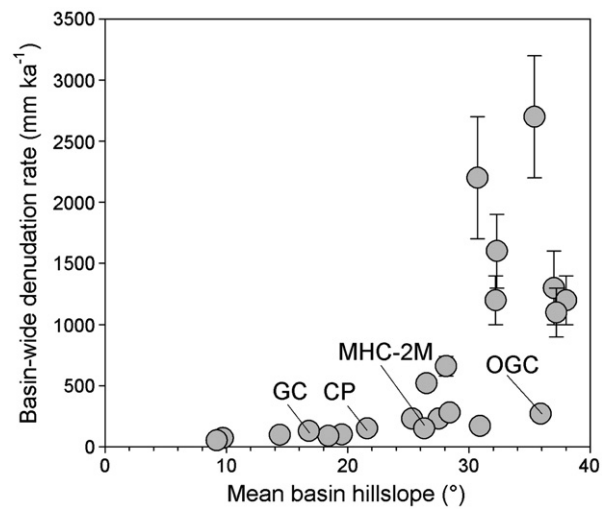


Fig. 4. The relationship between basin-wide denudation rates and mean basin hillslope gradients for the basins shown in Fig. 1B. The broadly linear relationship between slope gradient and denudation rate decouples as slopes exceed approximately 30°, suggesting the emergence of threshold topography above this slope gradient (adapted from Binnie et al., 2007). Note, the San Gorgonio block has experienced tilting, which may bias the mean basin hillslope gradient. The samples discussed in detail in the text (MHC-2M, OGC, CP and GC) are indicated.

and slow spring melt may be less effective than extreme rainfall events would be in driving denudation. If this pattern has prevailed in the recent past this could explain why denudation rates of basin MHC-2M are not higher, as a significant proportion of the precipitation it receives is snow, making the volumes of rainfall received by MHC-2M and GC very similar. However, a comparison of basins MHC-2M and CP, where mean annual precipitation values are similar ($890 \pm 180 \text{ mm a}^{-1}$, $820 \pm 160 \text{ mm a}^{-1}$, respectively) but the amounts falling as rain and snow are different ($610 \pm 120 \text{ mm a}^{-1}$ snowfall in basin MHC-2M and $370 \pm 70 \text{ mm a}^{-1}$ snowfall in basin CP) also reveals similar denudation rates (Table 2). As the basins selected display the greatest possible range of precipitation values in the San Bernardino Mountains we surmise that neither mean annual precipitation, nor the proportion of it falling as rain or snow, can alone explain the variation in denudation rates we observe in this study.

5. Discussion

In mountain settings, the spatial coincidence of high precipitation and rapid crustal deformation has prevented workers from assessing conclusively the individual importance of these factors in driving denudation rates (Whipple, 2009). The difficulties inherent in isolating key variables responsible for driving denudation rates is a particular problem in the San Bernardino Mountains where there is a general north–south increase in each of mean annual precipitation, rates of tectonic uplift, lithological resistance and hillslope gradients (Spotila et al., 2002). This coincidence prevents any simple assessment of cause and effect relationships which may exist between climate, tectonics and denudation rates. However, the survival of the pre-orogenic weathered granitic horizon on the upper slopes of the San Gorgonio block and on the Big Bear block plateau suggests that these regions have, to some degree, been isolated from any base-level changes that have occurred in response to uplift, and therefore that crustal displacement has had little influence on denudation rates where the weathered granitic horizon has survived. Whereas the comparisons between mean annual precipitation and denudation rates from throughout the mountains appear to show a broadly positive relationship (Fig. 3), these denudation rates must also embody the influence of base-level changes brought about by crustal displacement. The lack of a relationship between precipitation and denudation rates is only revealed in this study by comparing results from individual basins (GC, CP and MHC-2M) where the influence of crustal displacement can be constrained.

5.1. The controls of denudation rates on the Big Bear block plateau

Several other basins situated on the plateau of the Big Bear block, as well as CP and GC, retain mantles of the weathered granitic horizon over large portions of their surface (CLG, CRD, ARC). By comparing denudation rates over different timescales among basins on the plateau using cosmogenic ^{10}Be analysis ($\sim 10^4$ a) and by measuring the depth of incision into the pre-uplift horizon ($\sim 10^6$ a), Binnie et al. (2008) found a strong linear relationship and systematically greater rates measured over $\sim 10^4$ a timescales than those measured over $\sim 10^6$ a (Fig. 5). The increase in rates is not great (\sim two-fold), but of particular interest here is not the degree of difference rather the significance of the strong correlation between these two independent datasets. It is tempting to suggest climatic change as a cause for such a widespread systematic increase, however, the comparisons using rainfall and snowfall data in the three basins discussed above implies precipitation is not the principal control of denudation rates in this setting. Binnie et al. (2008) interpreted the systematically greater denudation rates over 10^4 a as compared to 10^6 a timescales (Fig. 5) as the lagged response of topography to the relative crustal uplift of the Big Bear block, implying that subsequent to the initial crustal displacement it was the upstream migration of channel incision and

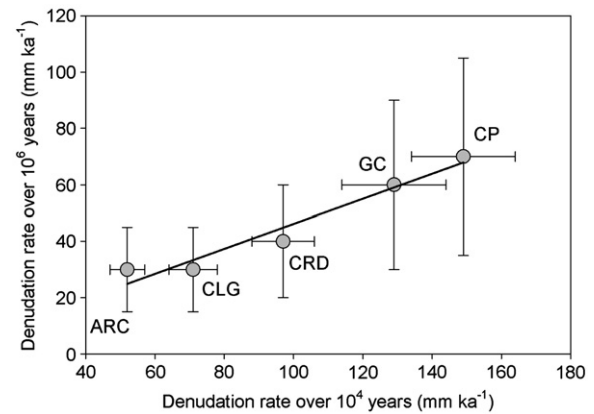


Fig. 5. Basin-wide denudation rates measured over different timescales from basins CP, CRD, CLG, GC, LLC and ARC on the Big Bear block, adapted from Binnie et al. (2008). Cosmogenic nuclide analysis gives denudation rates on timescales of 10^4 years (x-axis). Quantifying the depth of incision into a dated horizon allows denudation rates of the plateau surface to be derived for the past ~ 2.5 Ma, and the mean long-term denudation rate for each basin extracted (y-axis). The linear agreement shows denudation rates are systematically greater over 10^4 a timescales as compared to those measured over 10^6 a timescales.

the resulting steepening of hillslopes over time that has increased rates. In this scenario, rates will continue to increase until a more rugged topography is achieved and the slopes attain an equilibrium form with respect to local base level, assuming base level remains constant long enough for this to occur. The Big Bear block plateau may, therefore, be seen as an evolving landscape that is responding to the onset of orogenesis as it tends towards a topographic steady-state. If it is assumed that the steep, rapidly eroding southern regions of the San Bernardino Mountains have achieved topographic steady-state, whereby mean slope gradients remain relatively constant through time, then the evolution of the topography of the Big Bear block plateau towards a similar state can be envisaged by following the left to right trajectory of the points plotted in Fig. 4, although it cannot be assumed that tectonic displacement would be sufficiently large and channel incision rates sufficiently rapid for slopes to reach threshold angles for failure. A similar model of topographic evolution has been proposed for the San Bernardino Mountains by Spotila et al. (2002) and Spotila (2005), who note that the Big Bear block is in a transitional state where drainage is undergoing reorganisation and topography is tending towards a more dissected appearance, similar to that observed in the older San Gabriel Mountains to the west.

The comparison between precipitation and denudation rates for basins GC, CP and MHC-2M (Section 4), where the influence of crustal displacement can be constrained, suggests that denudation rates are not a direct function of precipitation, as suggested by the stream-power relationship. However, if, as suggested by stream-power modelling, rates of channel incision and knickpoint migration are related to discharge (Whipple and Tucker, 1999), then the role of precipitation would be to dictate the rate at which base-level changes, originating at the bounding faults of the Big Bear block, are communicated upstream from the catchment mouths around the periphery of the block towards the headwaters in the centre. This, in turn, would influence the length of time it takes young orogens to achieve topographic steady-state. Alternatively, if the Big Bear block were not so broad it would take less time to achieve equilibrium between slope form and channel incision (Anhert, 1984), and so during the early stages of fault block orogenesis the spatial distribution of major faults could also be seen as a primary control of denudation. Based on rates of plate convergence, Stolar et al. (2007) proposed that it has taken the mountain ranges of Taiwan 1.8–2.3 Ma after becoming sub-aerially exposed to achieve topographic steady-state; a finding that is consistent with model estimates that it takes the removal of three times the landscape relief to achieve a topographic steady-state

(Howard et al., 1994). A modelling study by Whipple and Meade (2006) provides comparable estimates of ~3–4 Ma for Taiwan to achieve mass-flux steady-state. If we assume uplift of the Big Bear block began in the Late Pliocene, our data imply that the northern San Bernardino Mountains will take longer to achieve either a topographic or mass flux steady-state, but that this period could be reduced by a wetter climate. This suggests that a better understanding of rates of knickpoint migration is crucial to determine what controls denudation in such settings, and highlights the importance of the spacing of structurally defined landscape discontinuities, such as block bounding faults, as key factors in the macro-scale pattern of denudation rates during the early stages of mountain building.

5.2. Controls of denudation rates in threshold topography

The southern San Bernardino Mountains generally display much steeper, more rugged topography than is found on the plateau further north, and rapid mass movement events in the form of rockfalls, shallow landslides and debris or mud flows are common (Sadler and Morton, 1989; Morton et al., 2008). The lack of a relationship between precipitation and denudation rate discussed in the previous section takes into account only catchments where rapid mass movement processes are not common. In this section the factors driving denudation rates are considered explicitly for those basins where slope failure is occurring.

5.2.1. Landslide driven denudation

It is important at this point to make a distinction between those mechanisms that drive denudation rates over the long term and those that may trigger a denudational 'event' in tectonically active settings. By increasing the shear stress and lowering shear strength, precipitation encourages slope failure. Correlations between precipitation and modern sediment yields have previously been recorded in high relief environments (Dadson et al., 2003). Keefer (1984) and Lavé and Burbank (2004) have proposed that the relative contribution to denudation rates from precipitation-induced landsliding in some mountain ranges of southern California is more significant than that caused by seismic shaking. However, while precipitation or earthquakes can trigger landslides, in order for slopes to retain their steepness and remain close to their threshold angle of stability they require continual incision at their toes (Burbank et al., 1996; Densmore et al., 1997). Either precipitation or seismic shaking might cause a landslide but for such events to persist over the longer-term necessitates continuous base-level lowering in order to restore the steepness of slope angles after failure. Prevailing climate, or lithology, may play a role in controlling the threshold angle at which slopes exist over the long-term (Schmidt and Montgomery, 1995; Gabet et al., 2004). However, once slopes have reached their threshold angle it is channel incision or relative vertical crustal offset across faults at the base of slopes that will drive denudation rates at the landscape scale (Binnie et al., 2007). This assertion assumes that landsliding is related in some way to slope angle and that slopes will fail only when they exceed some threshold value for stability. This is clearly not the case for many large landslides that have occurred in lower relief topography, such as the massive Blackhawk landslide on the northern range front of the San Bernardino Mountains. However, in such instances structural or lithological boundaries have typically facilitated failure (Korup et al., 2007) and so the discussion above can be considered valid at least where shallow sliding is dominant.

5.2.2. Sediment transport and denudation rate

By plotting mean slope angle against denudation rate for the San Bernardino Mountains it is apparent that when slope angles exceed ~30° there is a decoupling of the broadly linear relationship between slope angle and denudation rate (Fig. 4). This point marks the emergence of threshold topography, principally to the south, and is coincident with the transition from transport-limited to detachment-

limited denudation in the San Bernardino Mountains (Binnie et al., 2007). As the crustal blocks of the southern San Bernardino Mountains are defined by strands of the San Andreas Fault, then it follows that it must be either displacement on the block bounding faults or channel incision along Mill Creek that will steepen and maintain the threshold slopes of the Yucaipa Ridge and southern San Gorgonio blocks, and thus drive denudation rates. It is possible to evaluate the likelihood of these two scenarios using our denudation rate data.

The slopes of the Yucaipa Ridge block and southern slopes of the San Gorgonio block both have mean average gradients of 32° (based on USGS National Elevation Dataset 1/3-arcsecond DEM). The comparatively low denudation rate ($270 \pm 28 \text{ mm ka}^{-1}$) recorded from the steep topography of the southern San Gorgonio block by sample OGC contrasts sharply with the high rates from the similarly steep basins on the Yucaipa Ridge (between $2700 \pm 300 \text{ mm ka}^{-1}$ and $1100 \pm 200 \text{ mm ka}^{-1}$). If fluvial incision of the Mill Creek were driving denudation rates, by steepening the slopes of the northern Yucaipa Ridge and southern San Gorgonio blocks, then denudation rates on both sides of the valley would be similar (Fig. 6A). However, whereas the upper reaches of Mill Creek display evidence for fluvial incision (Spotila et al., 2002), the channel in the valley further downstream contains an appreciable amount of deposited fill material, a situation not indicative of a channel actively incising bedrock. This implies that channel incision at the foot of the slopes of the Yucaipa Ridge block is not driving the high rates of denudation recorded there and so a base-level drop induced by vertical crustal offset across a fault rather than fluvial incision must be maintaining the steepness of Yucaipa Ridge slopes (Fig. 6B). This is further supported by the lack of a trunk stream along the southern extents of the Yucaipa Ridge block that suggests these slopes are indeed able to be maintained at their threshold angle by displacement on the block bounding faults.

The evidence above suggests that displacement on the Mill Creek fault controls the rates of denudation of the valley side-slopes, and this assertion is supported by the sediment fill of Mill Creek which is not indicative of active bedrock channel incision. In the absence of channel incision this scenario could not operate over the long term without conspicuously raising the floor of the Mill Creek relative to where it exits the range front. One explanation for this apparent discrepancy is that the periodic evacuation of detritus from Mill Creek and subsequent periods of bedrock channel incision occur sufficiently frequently so as to allow the steep side-slopes of the Mill Creek to be maintained (Sadler and Morton, 1989). This suggests a role for precipitation in controlling the denudation rates of mountainous topography not by driving incision but by transporting deposited material. Without the periodic removal of the alluvial deposits and side-slope talus aprons deposited along the base of slopes of Mill Creek then downcutting of the main channel would not keep pace with base-level lowering and the valley-side slopes would over time become shallower and cease to be at threshold. Thus, maintenance of the tectonically-driven rates of denudation over the long-term requires a sufficient amount of precipitation to transport the denudational debris produced, implying that high rates of denudation can persist only when high rates of tectonic activity coincide with precipitation which is sufficient to move valley fill material. Having only one denudation rate result from the steep southern slopes of the San Gorgonio block makes this suggestion somewhat tentative (Binnie et al., 2008), although the process of bedrock channel incision following the excavation of fill deposits is compatible with notions of sediment flushing (Hovius et al., 2000; Miller and Benda, 2000) and sporadic denudation in mountain environments (Kirchner et al., 2001), and is also in accord with the idea that rapid rates of denudation result from timely combinations of tectonic and climatic events (Dadson et al., 2003).

5.2.3. The role of large, rare landslides

Whereas the highly fractured nature of the gneiss comprising the bedrock of the Yucaipa Ridge appears to prevent deep-seated

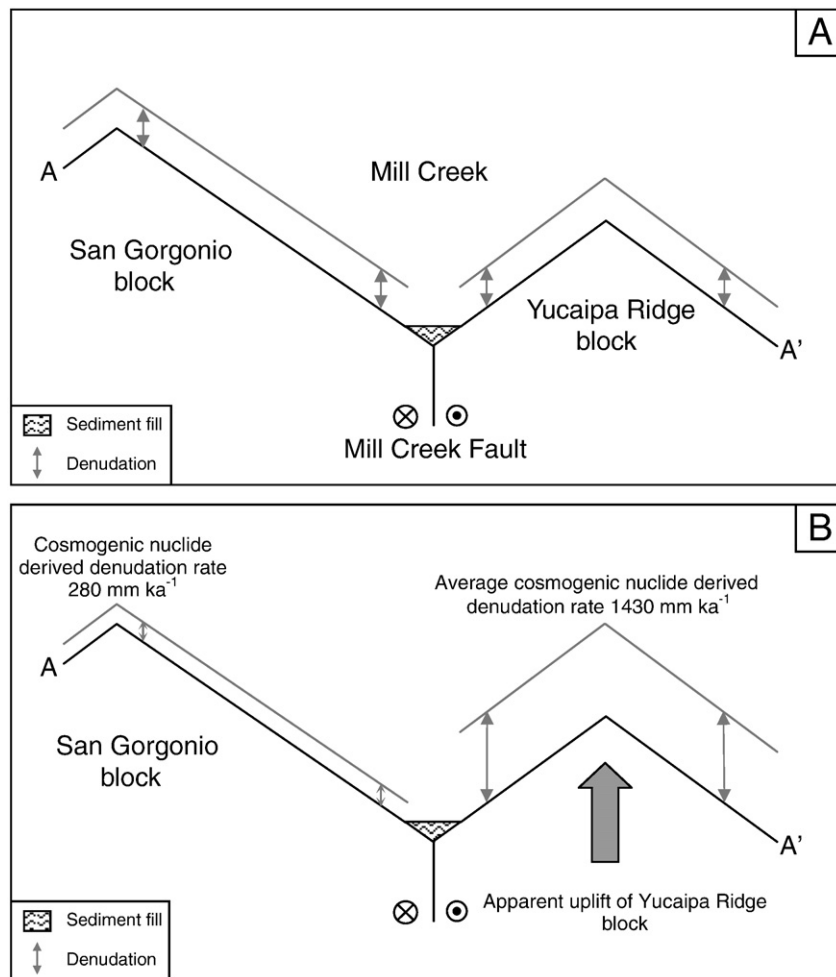


Fig. 6. (A) Simplified cross section A–A' (Fig. 1B) shows the hypothetical scenario which would be expected if incision of Mill Creek were driving the rates of denudation of the slopes of the San Gorgonio and Yucaipa Ridge block. Rates of denudation of the opposing valley slopes would, in this case, be similar. (B) The same cross section as in (A) but with the inclusion of the denudation rates of the basins draining into Mill Creek, as recorded in this study. The differences in rates on opposing sides of the valley suggests the Yucaipa Ridge block is experiencing crustal uplift relative to the San Gorgonio block, and that this uplift can account for the majority of the denudation of the Yucaipa Ridge block slopes. Thermochronometric cooling histories of Yucaipa Ridge suggest long-term denudation rates of between 800 and 1600 mm ka^{-1} (see Spotila et al., 2001; Binnie et al., 2008).

landsliding, the more competent quartz monzonite of the western San Gorgonio block is more likely to be able to sustain steep slopes for longer periods before failing. It is difficult to determine whether landsliding is currently an important agent of denudation on the southern slopes of the San Gorgonio block, although the rugged nature of the hillslopes and presence of topographic benches would suggest large landslides have occurred in the past. We cannot, therefore, discount a further explanation for the low denudation rate of the southern San Gorgonio block being that the mass flux here is dominated by rare, deep-seated landsliding. This process would not be recorded by cosmogenic radionuclide analysis if it occurred sufficiently rarely. Because of this the role of large landslides might be underestimated in our dataset. However, analyses of the contribution of large landslides to the overall rate of denudation suggests they typically would not explain the degree of difference in rates observed on opposing sides of the Mill Creek valley (Korup et al., 2007). Furthermore, thermochronometric ages from this region give long-term denudation rates that are also more rapid on the Yucaipa Ridge rather than on the San Gorgonio block (Spotila et al., 2002). These rates would incorporate any contribution from large landslides if they were occurring on the San Gorgonio block, implying that high magnitude low frequency landsliding is not the explanation for the variability in rates on opposing sides of the valley.

5.3. The importance of the averaging period of the measurement

A significant obstacle to the study of how climatic and tectonic influences can control landscape evolution is the different timescales over which they operate and the averaging time of the denudation rate measurements. The time required for tectonic processes to generate significant relief, or alter hillslope gradients, is probably several orders of magnitude greater than the typical 10^2 – 10^4 year averaging period of our cosmogenic nuclide denudation rate measurements. Thus, the ability of cosmogenic techniques to record the influence of large-scale crustal deformation on denudation rates is somewhat limited to a snapshot of processes that are operating over a much longer time frame, and any increase or decrease in the rate of crustal displacement is unlikely to be reflected in the denudation rates of the landscape over the timescales of cosmogenic measurements. As such, the denudation rates derived from the San Bernardino Mountains should be considered as existing within a tectonic regime which may be continuing, or which may have ceased or changed at some time in the past.

This point is relevant to our study for two reasons. Firstly, our interpretations of the variation in denudation rates between the Yucaipa Ridge and San Gorgonio blocks as resulting from a differential crustal uplift requires the denudation rate measurements to be

representative of processes operating over longer timescales. Secondly, it suggests that there may be a significant time lag between tectonic events, or changes in the long-term rates of crustal displacement, and their topographic impact. The survival of the weathered granite palaeosurface in the centre of the Big Bear block, and at high elevations on the San Gorgonio block, exemplifies this point and suggests that the rejuvenation resulting from the onset of orogenesis is continuing on the slopes of these blocks (Spotila et al., 2002; Binnie et al., 2008). Hence, constraining the influence of crustal displacement on landscape development using denudation rates derived from cosmogenic nuclide analysis must take into account that the rates measured may reflect a response to tectonic processes which operated several million years previously.

With regard to climate, the averaging period of cosmogenic nuclide-derived denudation rates embodies a different set of problems. Basin-averaged cosmogenic radionuclide-derived denudation rates are relatively insensitive to minor rate fluctuations, however, climate is likely to vary over the duration of the cosmogenic analysis (Viles and Goudie, 2003), meaning that modern precipitation is probably not an accurate representation of the mean precipitation over the averaging time of the denudation rate measurements. It is apparent that the climate has not been constant over the averaging periods of the denudation rates we derive in San Bernardino Mountains (Table 2) (Eppes et al., 2003; McDonald et al., 2003). The San Gorgonio block is the only site in southern California to have been glaciated during the Pleistocene and Holocene, and although glacial activity was limited to small cirque glaciers, readvances have been recorded at 18–20 ka, 16–15 ka, 12–13 ka and 5–9 ka mid-way along the northern flank of the ridge (Owen et al., 2003). In addition, the south-western United States, including the Mojave Desert, has experienced pluvial periods during the late Pleistocene and Holocene (Bull, 1991). However, the strong orographic rainshadow that presently exists has probably been a consistent feature since the San Gabriel Mountains migrated west along the San Andreas Fault and past the southern San Bernardino Mountains, and since the growth of the Yucaipa Ridge block. Also, the evidence for glacial activity on the crest of the San Gorgonio block suggests that it has been elevated sufficiently since at least the Late Pleistocene to induce precipitation in the south and impose a rainshadow in the north. Thus, while climatic changes may have influenced volumes of precipitation and the elevation of the snow-line, plus associated vegetation and wildfire frequencies, the gross pattern of higher precipitation in the south as compared to the north has probably been maintained over the averaging time of our denudation rate measurements. However, our conclusions regarding the lack of a climatic control remain tentative due to the lack of a detailed record of precipitation across the mountains throughout this time.

5.4. Broader implications for controls of denudation rates in orogens

In the San Bernardino Mountains we propose that high rates of denudation are a function of both rapid tectonic uplift and sufficient precipitation to evacuate denuded material. The need for fluvial transport to remove intermontane detritus in order to maintain rapid long-term denudation has been recognised by other studies (e.g. Thiede et al., 2004), while the convergence of multiple factors has been suggested as the driver of rapid decadal-scale denudation rates in Taiwan (Dadson et al., 2003). As noted above, the positive relationship between rapid tectonic uplift and high precipitation in mountainous regions is common, and makes it difficult to distinguish between the influences each has on the rates of denudation (Whipple, 2009; Spotila et al., 2002). By selecting settings where only one of either precipitation or uplift rates vary, workers have attempted to extract information regarding the control each variable exerts on denudation rates (e.g. Burbank et al., 2003; Reiners et al., 2003; Grujic et al., 2006). Issues relating to the averaging periods of the techniques used (see

Section 5.3 above), and the potential role for glacial erosion in some settings notwithstanding, the findings of these studies are contradictory. If rapid denudation rates are dependent on the co-variation of tectonic and climatic factors it becomes intractable, and perhaps meaningless, to measure the individual influence either has on denudation rates. Simple correlations between precipitation, uplift rate and denudation will not reveal cause and effect relationships if it is the timely interaction between precipitation and crustal uplift, rather than one or other of these variables, that is the fundamental denudation rate control. Whereas a gross relationship between precipitation and denudation rates may exist, our comparison from select basins suggests that in the San Bernardino Mountains precipitation is not a direct driver of rates. Rather, the results from Mill Creek imply that precipitation is required to facilitate the removal of denuded material, allowing crustal uplift to continue to drive denudation rates by restoring topography. If denudation rates in other high relief settings are controlled by the spatial coincidence of climatic and tectonic variables then there are implications for the hypothesis that climate-induced denudation regulates crustal deformation. It follows that one of the keys to understanding denudation rate controls in orogens is not simply comparisons of rates of uplift, precipitation and denudation. Future work is required to examine how precipitation drives sediment transport out of mountainous regions and how this transport might influence denudation rates.

6. Conclusions

Basin-wide denudation rates recorded in the San Bernardino Mountains vary approximately fifty-fold along a north–south transect. In those basins where the existence of pre-uplift topography suggests that the influence of crustal displacement on landscape evolution has been minimal, rates of modern mean annual precipitation do not correspond to basin-wide denudation rates. Instead, we propose that patterns of crustal displacement are the first-order control on such large variations in denudation rates over the temporal and spatial scales of our analysis. In the southern San Bernardino Mountains threshold hillslopes are maintained by bedrock uplift, but we hypothesise that volumes of precipitation underpin the ability of the fluvial system to evacuate denuded valley fill and so precipitation may regulate the ability of fault displacement to continue to drive denudation rates. The northern regions of the mountains are dominated by low relief topography that is still responding to the orogenesis that began several millions of years ago. The amount of time that elapses before denudation rates of basins at the centre of crustal blocks equilibrate with new rates of base-level lowering around the block periphery depends on the dimensions of the block and the length of time it takes changes to be communicated through the landscape. Hence, while crustal displacement dictates the potential magnitude of denudation rates, it may be a combination of precipitation and fault spacing that controls the time it takes for this response to be felt in different parts of a mountain range. Our findings suggest that, in rapidly and more moderately denuding mountain ranges, rates of denudation are controlled by the coincidence of tectonic and climatic factors. Such considerations of the different ways in which precipitation might facilitate denudation rates in tectonically active settings, alongside a recognition that the averaging periods of measurements may need to be accounted for in comparisons of denudation and precipitation, are critical to developing a more detailed understanding of what drives denudation rates and topographic evolution in orogens.

Acknowledgements

This work was funded by a NERC research studentship awarded to Binnie (NER/S/A/2000/03335). Summerfield acknowledges support from the Carnegie Trust for the Universities of Scotland. Comments by

Andrew Plater, Mike Kaplan and two anonymous reviewers significantly improved an earlier version of this manuscript. We thank A. Davidson; L. Nicholson and C. Cook for fieldwork and laboratory assistance. The Southern California Audubon Society kindly granted access to Yucaipa Ridge.

References

- Allen, C.R., 1957. San Andreas fault zone in San Geronio Pass, southern California. *Geological Society of America Bulletin* 68, 315–349.
- Anhert, F., 1984. Local relief and the height limits of mountain ranges. *American Journal of Science* 284, 1035–1055.
- Balco, G., Stone, J.O., Lifton, N.A., Dunai, T.J., 2008. A complete and easily accessible means of calculating surface exposure ages or erosion rates from ^{10}Be and ^{26}Al measurements. *Quaternary Geochronology* 3, 174–195.
- Binnie, S.A., Phillips, W.M., Summerfield, M.A., Fifield, L.K., 2006. Sediment mixing and basin-wide cosmogenic nuclide analysis in rapidly eroding mountainous environments. *Quaternary Geochronology* 1, 4–14.
- Binnie, S.A., Phillips, W.M., Summerfield, M.A., Fifield, L.K., 2007. Tectonic uplift, threshold hillslopes, and denudation rates in a developing mountain range. *Geology* 35, 743–746.
- Binnie, S.A., Phillips, W.M., Summerfield, M.A., Fifield, L.K., Spotila, J.A., 2008. Patterns of denudation through time in the San Bernardino Mountains, California: implications for early-stage orogenesis. *Earth and Planetary Science Letters* 275, 62–72.
- Brown, E.T., Stallard, R.F., Larsen, M.C., Raisbeck, G.M., 1995. Denudation rates determined from the accumulation of in situ-produced ^{10}Be in the Luquillo Experimental Forest, Puerto Rico. *Earth and Planetary Science Letters* 129, 193–202.
- Bull, W.B., 1991. *Geomorphic responses to climatic change*. Oxford Univ. Press, New York, NY.
- Burbank, D.W., Leland, J., Fielding, E., Anderson, R.S., Brozovic, N., Reid, M.R., Duncan, C., 1996. Bedrock incision, rock uplift and threshold hillslopes in the northwestern Himalayas. *Nature* 379, 505–510.
- Burbank, D.W., Blythe, A.E., Putkonen, J., Pratt-Sitaula, B., Gabet, E., Oskin, M., Barros, A., Ojha, T.P., 2003. Decoupling of erosion and precipitation in the Himalayas. *Nature* 426, 652–655.
- Cox, B.F., Hillhouse, J.W., Owen, L.A., 2003. Pliocene and Pleistocene evolution of the Mojave River, and associated tectonic development of the Transverse Ranges and Mojave Desert, based on borehole stratigraphy studies and mapping of landforms and sediments near Victorville, California. In: Enzel, Y., Wells, S.G., Lancaster, N. (Eds.), *Paleoenvironments and Paleohydrology of the Mojave and Southern Great Basin Deserts: Special Paper*, vol. 368. Geological Society of America, Boulder, CO, pp. 1–42.
- Dadson, S.J., Hovius, N., Chen, H., Dade, B., Hsieh, M.L., Willett, S.D., Hu, J.C., Horng, M.J., Chen, M.C., Stark, C.P., Lague, D., Lin, J.C., 2003. Links between erosion, runoff variability and seismicity in the Taiwan Orogen. *Nature* 426, 648–651.
- Densmore, A.L., Anderson, R.S., McAadoo, B.G., Ellis, M.A., 1997. Hillslope evolution by bedrock landslides. *Science* 275, 369–372.
- Dibblee, J.R., 1982. *Geology of the San Bernardino Mountains, Southern California*. In: Fife, D.L., Minch, J.A. (Eds.), *Geology and mineral wealth of the California Transverse Ranges; Mason Hill volume*. South Coast Geol. Soc., University of California, pp. 148–169.
- Dunne, J., Elmore, D., Muzikar, P., 1999. Scaling factors for the rates of production of cosmogenic nuclides for geometric shielding and attenuation at depth on sloped surfaces. *Geomorphology* 27, 3–11.
- Eppes, M.C., McDonald, E.V., McFadden, L.D., 2003. Soil geomorphological studies in the Mojave Desert; impacts of Quaternary tectonics, climate, and rock type on soils, landscapes, and plant-community ecology. In: Easterbrook, D.J. (Ed.), *Quaternary geology of the United States; INQUA 2003 field guide volume*. Desert Research Institute, Reno, NV, pp. 105–122.
- Ferrier, K.L., Kirchner, J.W., Finkel, R.C., 2005. Erosion rates over millennial and decadal timescales at Caspar Creek and Redwood Creek, Northern California Coast Ranges. *Earth Surface Processes and Landforms* 30, 1025–1038.
- Gabet, E.J., Pratt-Sitaula, B.A., Burbank, D.W., 2004. Climatic controls on hillslope angle and relief in the Himalayas. *Geology* 32, 629–632.
- Gosse, J.C., Phillips, F.M., 2001. Terrestrial in situ cosmogenic nuclides: theory and application. *Quaternary Science Reviews* 20, 1475–1560.
- Granger, D.E., Riebe, C.S., Kirchner, J.W., Finkel, R.C., 2001. Modulation of erosion on steep granitic slopes by boulder armoring, as revealed by cosmogenic ^{26}Al and ^{10}Be . *Earth and Planetary Science Letters* 186, 269–281.
- Grujic, D., Coutand, I., Bookhagen, B., Bonnet, S., Blythe, A., Duncan, C., 2006. Climatic forcing of erosion, landscape, and tectonics in the Bhutan Himalayas. *Geology* 34, 801–804.
- Harris, S.E., Mix, A.C., 2002. Climate and tectonic influences on continental erosion of tropical South America, 0–13 Ma. *Geology* 30, 447–450.
- Hartshorn, K., Hovius, N., Dade, W.B., Slingerland, R.L., 2002. Climate-driven bedrock incision in an active mountain belt. *Science* 297, 2036–2038.
- Hovius, N., 2000. Macroscale process systems of mountain belt erosion. In: Summerfield, M.A. (Ed.), *Geomorphology and Global Tectonics*. John Wiley Sons, Chichester, pp. 77–108.
- Hovius, N., Stark, C.P., Hao-Tsu, C., Jiun-Chuan, L., 2000. Supply and removal of sediment in a landslide-dominated mountain belt: Taiwan. *Journal of Geology* 108, 73–89.
- Howard, A.D., Kerby, G., 1983. Channel changes in badlands. *Geological Society of America Bulletin* 94, 739–752.
- Howard, A.D., Dietrich, W.E., Seidl, M.A., 1994. Modeling fluvial erosion on regional to continental scales. *Journal of Geophysical Research* 99, 13,971–13,986.
- Huntington, K.W., Blythe, A.E., Hodges, K.V., 2006. Climate change and late Pliocene acceleration of erosion in the Himalaya. *Earth and Planetary Science Letters* 252, 107–118.
- Keefer, D.K., 1984. Landslides caused by earthquakes. *Geological Society of America Bulletin* 95, 406–421.
- Kirchner, J.W., Finkel, R.C., Riebe, C.S., Granger, D.E., Clayton, J.L., King, J.G., Megahan, W.F., 2001. Mountain erosion over 10 yr, 10 ky., and 10 m.y. time scales. *Geology* 29, 591–594.
- Kohl, C.P., Nishiizumi, K., 1992. Chemical isolation of quartz for measurement of in situ-produced cosmogenic nuclides. *Geochimica et Cosmochimica Acta* 56, 3583–3587.
- Korup, O., Clague, J.J., Hermanns, R.L., Hewitt, K., Strom, A.L., Weidinger, J.T., 2007. Giant landslides, topography, and erosion. *Earth and Planetary Science Letters* 261, 578–589.
- Lavé, J., Burbank, D., 2004. Denudation processes and rates in the Transverse Ranges, Southern California; erosional response of a transitional landscape to external and anthropogenic forcing. *Journal of Geophysical Research* 109, F101006.
- Malusa, M.G., Vezzoli, G., 2006. Interplay between erosion and tectonics in the Western Alps. *Terra Nova* 18, 104–108.
- May, S.R., Repenning, C.A., 1982. New evidence for the age of the Old Woman Sandstone, Mojave Desert, California. In: Cooper, J.D. (Ed.), *Geologic excursions in the Transverse Ranges, southern California: volume and guidebook*. Geological Society of America, Boulder CO, pp. 93–96.
- McDonald, E.V., McFadden, L.D., Wells, S.G., 2003. Regional response of alluvial fans to the Pleistocene–Holocene climatic transition, Mojave Desert, California. In: Enzel, Y., Wells, S.G., Lancaster, N. (Eds.), *Paleoenvironments and Paleohydrology of the Mojave and Southern Great Basin Deserts: Special Paper*, vol. 368. Geological Society of America, Boulder, CO, pp. 189–205.
- Meisling, K.E., Weldon, R.J., 1989. Late Cenozoic tectonics of the northwestern San Bernardino Mountains, Southern California. *Geological Society of America Bulletin* 101, 106–128.
- Middleton, R., Klein, J., 1987. *AI-26 – Measurement and Applications*. Philosophical Transactions of the Royal Society of London Series A-Mathematical Physical and Engineering Sciences 323, 121–143.
- Miles, S.R., Goudie, C.B., 1997. *Ecological subregions of California, Section and subsection descriptions*. USDA Forest Service Pacific Southwest Region, San Francisco, CA. R5-EM-TP-005.
- Miller, D.J., Benda, L.E., 2000. Effects of punctuated sediment supply on valley-floor landforms and sediment transport. *Geological Society of America Bulletin* 112, 1814–1824.
- Minnich, R.A., 1986. Snow levels and amounts in the mountains of Southern California. *Journal of Hydrology* 89, 37–58.
- Minnich, R.A., 1989. Climate, fire and landslides in Southern California. Landslides in a semi-arid environment with emphasis on the inland valleys of Southern California. *Publications of the Inland Geological Society* 2, 91–100.
- Montgomery, D.R., Balco, G., Willett, S.D., 2001. Climate, tectonics, and the morphology of the Andes. *Geology* 29, 579–582.
- Morton, D.M., Alvarez, R.M., Ruppert, K.R., Goforth, B., 2008. Contrasting rainfall generated debris flows from adjacent watersheds at Forest Falls, southern California, USA. *Geomorphology* 96, 322–338.
- Niemi, N.A., Oskin, M., Burbank, D.W., Heimsath, A.M., Gabet, E.J., 2005. Effects of bedrock landslides on cosmogenically determined erosion rates. *Earth and Planetary Science Letters* 237, 480–498.
- Oberlander, T.M., 1972. Morphogenesis of granitic boulder slopes in the Mojave Desert, California. *Journal of Geology* 80, 1–20.
- Owen, L.A., Finkel, R.C., Minnich, R.A., Perez, A.E., 2003. Extreme southwestern margin of late Quaternary glaciation in North America: timing and controls. *Geology* 31, 729–732.
- Reiners, P.W., Ehlers, T.A., Mitchell, S.G., Montgomery, D.R., 2003. Coupled spatial variations in precipitation and long-term erosion rates across the Washington Cascades. *Nature* 426, 645–647.
- Riebe, C.S., Kirchner, J.W., Granger, D.E., 2001a. Quantifying quartz enrichment and its consequences for cosmogenic measurements of erosion rates from alluvial sediment and regolith. *Geomorphology* 40, 15–19.
- Riebe, C.S., Kirchner, J.W., Granger, D.E., Finkel, R.C., 2001b. Minimal climatic control on erosion rates in the Sierra Nevada, California. *Geology* 29, 447–450.
- Sadler, P.M., Morton, D.M., 1989. Landslides in the uppermost Santa Ana Basin and the adjacent San Bernardino Mountains of Southern California. In: Sadler, P.M., Morton, D.M. (Eds.), *Landslides in a semi-arid environment with emphasis on the inland valleys of Southern California*. The Inland Geological Society, Redland, CA, pp. 356–386.
- Sadler, P.M., Reeder, W.A., 1983. Upper Cenozoic, quartzite-bearing gravels of the San Bernardino Mountains, Southern California; recycling and mixing as a result of transpressional uplift. In: Andersen, D.W., Rymer, M.J. (Eds.), *Tectonics and Sedimentation Along the Faults of the San Andreas System*. Society of Economic Paleontologists and Mineralogists, Pacific Section, Los Angeles, CA, pp. 45–57.
- Schmidt, K.M., Montgomery, D.R., 1995. Limits to relief. *Science* 270, 617–620.
- Seidl, M.A., Dietrich, W.E., Kirchner, J.W., 1994. Longitudinal profile development into bedrock; an analysis of Hawaiian channels. *Journal of Geology* 102, 457–474.
- Spotila, J.A., 2005. Applications of low-temperature thermochronometry to quantification of recent exhumation in mountain belts. *Reviews in Mineralogy and Geochemistry* 58, 449–466.
- Spotila, J.A., Sieh, K., 2000. Architecture of transpressional thrust faulting in the San Bernardino Mountains, Southern California, from deformation of a deeply weathered surface. *Tectonics* 19, 589–615.
- Spotila, J.A., Farley, K.A., Sieh, K., 1998. Uplift and erosion of the San Bernardino Mountains associated with transpression along the San Andres fault, California, as constrained by radiogenic helium thermochronometry. *Tectonics* 17, 360–378.

- Spotila, J.A., Farley, K.A., Douglas, Y.J., Reiners, P.W., 2001. Near-field transpressive deformation along the San Andreas fault zone in Southern California, based on exhumation constrained by (U–Th)/He dating. *Journal of Geophysical Research* 106, 30,909–30,922.
- Spotila, J.A., House, M.A., Blythe, A.E., Niemi, N.A., Bank, G.C., 2002. Controls on the erosion and geomorphic evolution of the San Bernardino and San Gabriel Mountains, Southern California. In: Barth, A. (Ed.), *Contributions to Crustal Evolution of the Southwestern United States: Special Paper*, vol. 365. Geological Society of America, Boulder, CO, pp. 205–230.
- Stolar, D.B., Willett, S.D., Montgomery, D.R., 2007. Characterization of topographic steady state in Taiwan. *Earth and Planetary Science Letters* 261, 421–431.
- Stone, J.O., 2000. Air pressure and cosmogenic isotope production. *Journal of Geophysical Research-Solid Earth* 105, 23,753–23,759.
- Thiede, R.C., Bookhagen, B., Arrowsmith, J.R., Sobel, E.R., Strecker, M.R., 2004. Climatic control on rapid exhumation along the Southern Himalayan Front. *Earth and Planetary Science Letters* 222, 791–806.
- Vance, D., Bickle, M., Ivy-Ochs, S., Kubik, P.W., 2003. Erosion and exhumation in the Himalaya from cosmogenic isotope inventories of river sediments. *Earth and Planetary Science Letters* 206, 273–288.
- Viles, H.A., Goudie, A.S., 2003. Interannual, decadal and multidecadal scale climatic variability and geomorphology. *Earth-Science Reviews* 61, 105–131.
- Whipple, K.X., 2009. The influence of climate on the tectonic evolution of mountain belts. *Nature Geoscience* 2, 97–104.
- Whipple, K.X., Tucker, G.E., 1999. Dynamics of the stream–power river incision model; implications for height limits of mountain ranges, landscape response timescales, and research needs. *Journal of Geophysical Research, B, Solid Earth and Planets* 104, 17,661–17,674.
- Whipple, K.X., Meade, B.J., 2006. Orogen response to changes in climatic forcing. *Earth and Planetary Science Letters* 243, 218–228.
- Whittaker, A.C., Cowie, P.A., Attal, M., Tucker, G.E., Roberts, G.P., 2007. Bedrock channel adjustment to tectonic forcing; implications for predicting river incision rates. *Geology* 35, 103–106.
- Wobus, C.W., Hodges, K.V., Whipple, K.X., 2003. Has focused denudation sustained active thrusting at the Himalayan topographic front? *Geology* 31, 861–864.
- Woodburne, M.O., 1975. *Cenozoic stratigraphy of the Transverse Ranges and adjacent areas, southern California*. Geological Society of America, Boulder, CO.
- Yule, D., Sieh, K., 2003. Complexities of the San Andreas Fault near San Geronio Pass; implications for large earthquakes. *Journal of Geophysical Research* 108 ETG 9-1-ETG 9-23.